

図3 PND13 - 18 の仔ラットの海馬 CA1 領域から得られた錐体細胞の刺激応答性

対照群の開眼日齢である PND16 を境に前半期 (PND13 - 15) と後半期 (PND16 - 18) に分けて、活動電位を発生させた細胞数を反映する集合スパイク電位の振幅 (PS amplitude、上段) とシナプス入力である集合シナプス後電位の傾き (fEPSP slope、下段) をまとめた。PND13 - 15 の時期では、fEPSP slope と、PS amplitude の電気刺激に対する応答性がともに VPA300 群において亢進していることが認められた ($p < 0.01$, repeated measure ANOVA)。一方、PND16 - 18 では、対照群と VPA300 群との間に有意差は認められなかった。

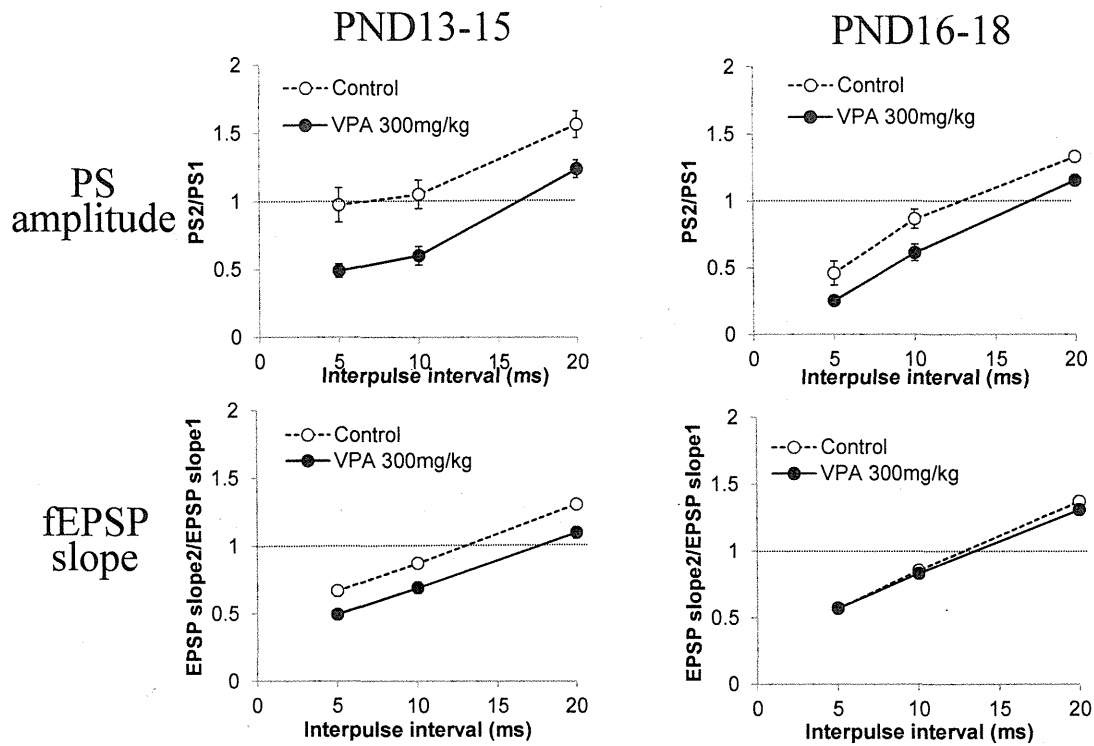


図4 フィードバック抑制に対する VPA 胎生期曝露の影響

仔ラット日齢を前半期 (PND13 - 15) と後半期(PND16 - 18)に分けて、GABA 神経細胞から錐体細胞の細胞層と先端樹状突起のシナプス層へのフィードバック抑制の強さを示した。横軸はダブルパルスの刺激間隔を、縦軸はペア応答比を示している。前半期において、細胞層 (PS amplitude ペア応答比) とシナプス層 (fEPSP slope ペア応答比) への GABA 作動性フィードバック抑制はいずれも VPA300 群において亢進していることが認められた ($p < 0.01$, repeated measure ANOVA)。後半期においては、細胞層への抑制の亢進は引き続き認められたが、シナプス層への抑制については対照群と有意差が認められなかった。

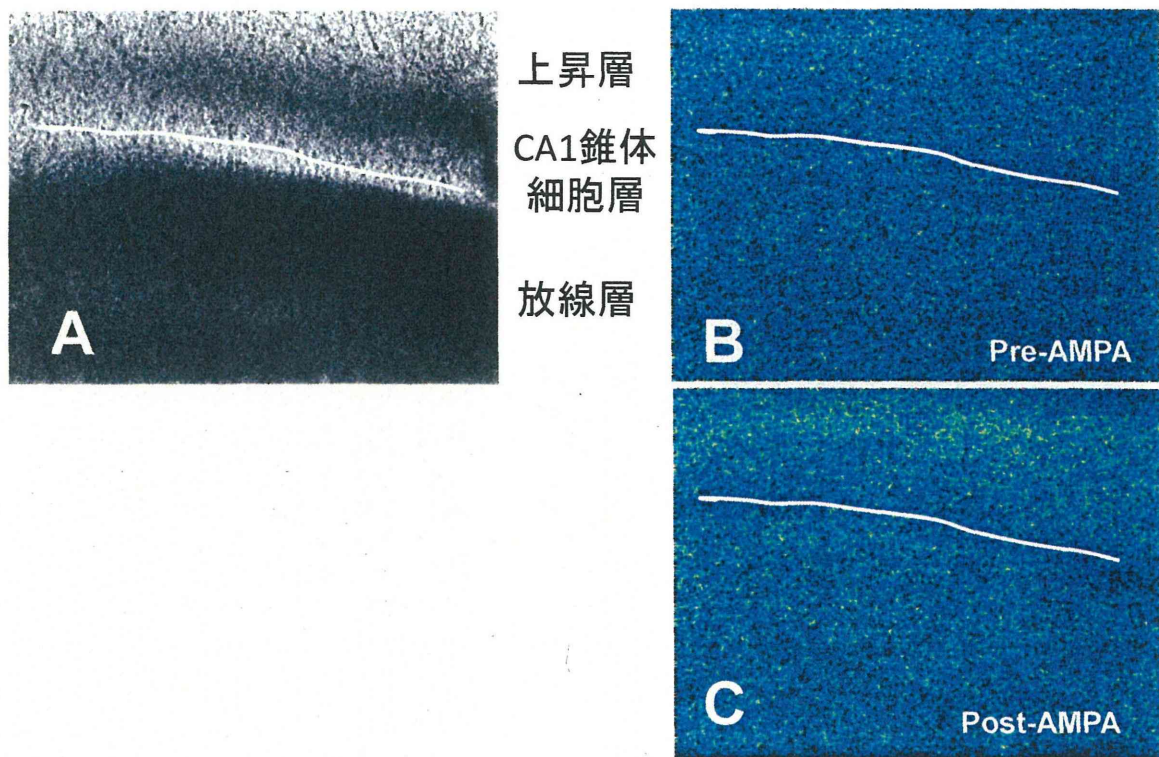


図5 対照群・PND14の海馬CA1領域においてAMPA (10 μ M)で誘発されたGABA放出の分布

A、海馬CA1領域の位相差光顕像。B、AMPA投与前のGABAの分布。C、AMPA投与45秒後のGABAの空間分布。AMPA投与で誘発された正味のGABAの放出分布はCの輝度からBの輝度を差し引いたものとなる。白い線は錐体細胞の位置を示す。3枚の像とも、上から上昇層、錐体細胞層、放線層である。AMPAによって上昇層のGABA分布に亢進している様子が観察される。

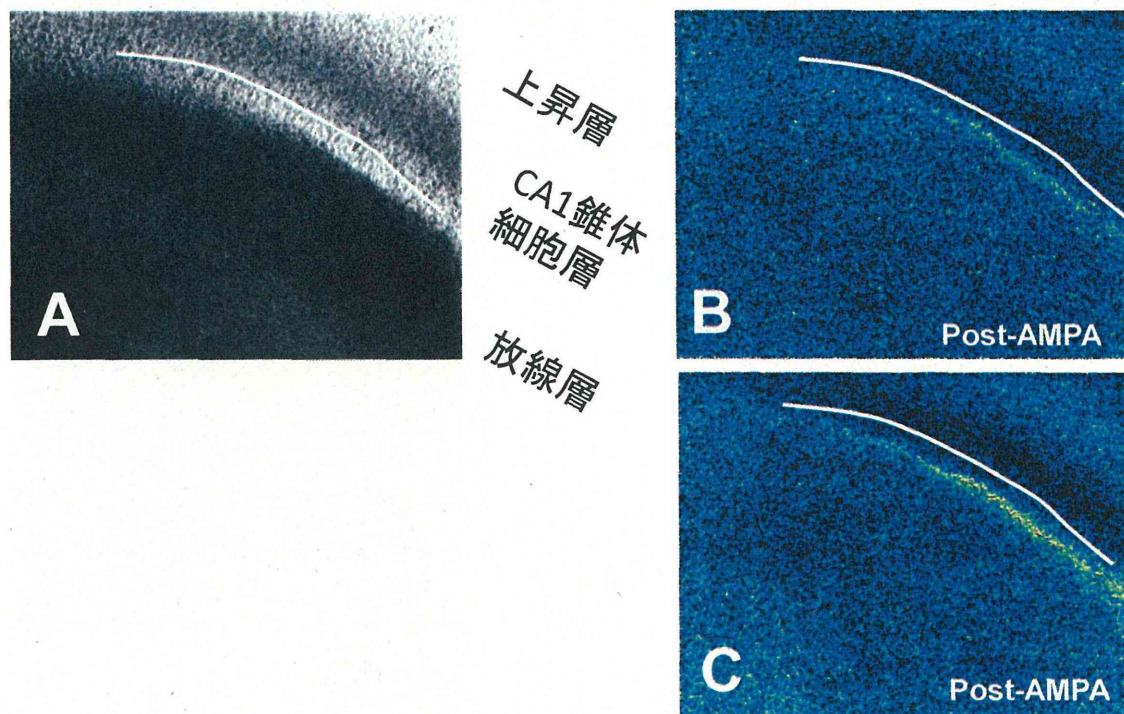


図6 VPA600群・PND13の仔ラットの海馬CA1領域においてAMPA (10 μ M)で誘導されたGABA放出分布

A、海馬CA1領域の位相差光顕像。B、AMPA投与前のGABAの分布。C、AMPA投与45秒後のGABAの空間分布。AMPA投与で誘導された正味のGABAの放出分布はCの輝度からBの輝度を差し引いたものとなる。白い線は錐体細胞の位置を示す。3枚の像とも、上から上昇層、錐体細胞層、放線層である。VPA600群ではAMPAによって錐体細胞層の下端にGABA分布が亢進している様子が観察された。対照群と比較すると、VPA600群ではGABAの放出分布が細胞層下端に局在していたケースが多かった。

III. 研究成果の刊行物に関する一覧表

研究成果の刊行に関する一覧表

雑誌

発表者氏名	論文タイトル名	発表誌名	巻号	ページ	出版年
Ishida K., Kotake Y., Miyara M., Aoki K., Sanoh S., Kanda Y., Ohta S.	Involvement of GluR2 decrease in lead-induced neuronal cell death.	<i>J. Toxicol. Sci.</i>	38	513-521	2013
Yamada S., Kotake Y., Sekino Y. and Kanda Y.	AMP-activated protein kinase-mediated glucose transport as a novel target of tributyltin in human embryonic carcinoma cells.	<i>Metallomics</i>	5	484-491	2013
Usami M., Mitsunaga K. Irie T., Miyajima A. and Doi O.	Proteomic analysis of ethanol-induced embryotoxicity in cultured post-implantation rat embryos.	<i>J. Toxicol. Sci.</i>	39	285-292	2014
Usami M., Mitsunaga K. Irie T. and Nakajima M.	Various definitions of reproductive indices: a proposal for combined use of brief definitions.	<i>Congenit. Anom.</i>	54	67-68	2014
Shigemoto-Mogami Y., Hoshikawa K., Goldman J., Sekino Y. and Sato K	Microglia enhance neurogenesis and oligodendrogenesis in the early postnatal subventricular zone.	<i>J. Neurosci.</i>	34 (5)	2231- 2243	2014
Takahashi K., Ishii-Nozawa R., Takeuchi K., Nakazawa K., Sekino Y. and Sato K.	Niflumic acid activates additional currents of the human glial L-glutamate transporter EAAT1 in a substrate-dependent manner.	<i>Biol. Pharm. Bull.</i>	36 (12)	1996- 2004	2013
Oguchi-Katayama A., Monma A., Sekino Y., Moriguchi T. and Sato K.	Comparative gene expression analysis of the amygdalae of juvenile rats exposed to valproic acid at prenatal and postnatal stages.	<i>J. Toxicol. Sci.</i>	38(3)	381-402	2013
Kinoshita M., Nasu-Tada K., Fujishita K., Sato K. and Koizumi S.	Secretion of matrix metalloproteinase-9 from astrocytes by inhibition of Tonic P2Y14-receptor-mediated signal(s).	<i>Cell. Mol. Neurobiol.</i>	33(1)	47-58	2013
Okura D., Horishita T., Ueno S., Yanagihara N., Sudo Y., Uezono Y., Sata T.	The endocannabinoid anandamide inhibits voltage-gated sodium channels Nav1.2, Nav1.6, Nav1.7 and Nav1.8 in <i>Xenopus</i> oocytes.	<i>Anesth. Analg.</i>	118	554-562	2014

Yanagihara N., Zhang H., Toyohira Y., Takahashi K., Ueno S., Tsutsui M., Takahashi K.	New insights into the pharmacological potential of plant flavonoids in the catecholamine system.	<i>J. Pharmacol. Sci.</i>	124	123-128	2014
Inagaki H., Toyohira Y., Takahashi K., Ueno S., Obara G., Kawagoe T., Tsutsui M., Hachisuga T., Yanagihara N.	Effects of selective estrogen receptor modulators on plasma membrane estrogen receptors and catecholamine synthesis and secretion in cultured bovine adrenal medullary cells.	<i>J. Pharmacol. Sci.</i>	124	66-75	2014
上野 晋	化学物質（金属・有機溶剤）の毒性学と産業医としての対応	産業医科大学雑誌	35 特集号	91-96	2013
Park EK, Wilson D, Choi HJ, Wilson CT, Ueno S.	Hazardous metal pollution in the republic of Fiji and the need to elicit human exposure.	<i>Environ Health Toxicol.</i>		doi:10.5620/eht.2013.28.e2013017	2013
Obara G., Toyohira Y., Inagaki H., Takahashi K., Horishita T., Kawasaki T., Ueno S., Tsutsui M., Sata T., Yanagihara N.	Pentazocine inhibits norepinephrine transporter function by reducing its surface expression in bovine adrenal medullary cells.	<i>J. Pharmacol. Sci.</i>	121	138-147	2013

書籍

著者氏名	論文タイトル名	書籍全体の編集者名	書籍名	出版社名	出版地	出版年	ページ
諫田泰成	再生心筋細胞を用いた安全性薬理評価系の開発	エイブル株式会社 和田昌憲	再生医療における臨床研究と製品開発	株式会社技術情報協会	東京都品川区	2013	572-576

IV. 研究成果の刊行物・別刷

Original Article

Involvement of decreased glutamate receptor subunit GluR2 expression in lead-induced neuronal cell death

Keishi Ishida¹, Yaichiro Kotake¹, Masatsugu Miyara¹, Kaori Aoki¹, Seigo Sanoh¹,
Yasunari Kanda² and Shigeru Ohta¹

¹Graduate School of Biomedical and Health Sciences, Hiroshima University,
1-2-3 Kasumi, Minami-ku, 734-8553, Japan

²Division of Pharmacology, National Institute of Health Sciences,
1-18-1, Kamiyoga, Setagaya-ku 158-8501, Japan

(Received April 4, 2013; Accepted April 25, 2013)

ABSTRACT — Lead is known to induce neurotoxicity, particularly in young children, and GluR2, an AMPA-type glutamate receptor subunit, plays an important role in neuronal cell survival. Therefore, we hypothesized that altered GluR2 expression plays a role in lead-induced neuronal cell death. To test this idea, we investigated the effect of exposure to 5 and 20 μM lead for 1-9 days on the viability and GluR2 expression of primary-cultured rat cortical neurons. The number of trypan-blue stained cells was increased by exposure to 5 μM lead for 9 days or 20 μM lead for 7-9 days, and LDH release was increased after exposure to 20 μM lead for 9 days. GluR2 expression was reduced by exposure to 5-100 μM lead, but not 0.1-1 μM lead, for 9 days. Immunocytochemistry also confirmed that GluR2 expression was decreased in the presence of lead. Application of 50 ng/ml brain-derived neurotrophic factor (BDNF) led to a recovery of lead-induced neuronal cell death, accompanied with increased GluR2 expression. Our results suggest that long-term exposure to lead induces neuronal cell death, in association with a decrease of GluR2 expression.

Key words: Lead, GluR2, Brain-derived neurotrophic factor

INTRODUCTION

Lead has been widely used in many products; for example, leaded gasoline, lead-based paint, and cans containing foods or alcoholic beverages. Exposure to high levels of environmental lead causes various public health problems, particularly among young children, because of its effects on the blood and brain, including disruption of nervous system communication (Gracia and Snodgrass, 2007). Recently, regulation of industrial and environmental levels of lead has been strengthened in many countries, but soil and water contamination is a persistent source of lead exposure in industrialized societies. Toxicity typically results from ingestion of food or water contaminated with lead, but may also occur after accidental ingestion of contaminated dust, soil, or lead-containing paints (Gracia and Snodgrass, 2007). Over 90% of lead absorbed after inhalation or oral ingestion is retained in the body and distributed to the bones (Links *et al.*, 2001), where the half-life of lead is decades long. It was reported that indi-

viduals with baseline blood lead levels of 10 to 19 $\mu\text{g}/\text{dl}$ suffer increased mortality from various causes: for example, mortality due to circulatory disease was increased by 10% and mortality due to cancer was increased by 46% relative to individuals with blood lead levels of less than 10 $\mu\text{g}/\text{dl}$ (Lustberg and Silbergeld, 2002). Thus, blood lead level is positively associated with mortality due to circulatory disorders and cancers.

Lead is known to induce neurotoxicity, leading to lowered intelligence test scores, behavioral problems and decreased cognitive ability (Canfield *et al.*, 2004; Laidlaw *et al.*, 2005). Lead-related intellectual deficits are seen in children with blood lead levels of at least 10 $\mu\text{g}/\text{dl}$, though no evidence of a threshold was found (Lanphear *et al.*, 2005). Schoolchildren with elevated blood lead levels due to both pre- and postnatal lead exposure are more likely to exhibit disruptive behavior in class (Leviton *et al.*, 1993; Bellinger *et al.*, 1994). Moreover, childhood exposure to lead is a risk factor for attention-deficit/hyperactivity disorder (ADHD) (Froehlich *et al.*,

Correspondence: Yaichiro Kotake (E-mail: yaichiro@hiroshima-u.ac.jp)

2009). However, the mechanisms involved have not been clarified in detail.

Glutamate is an essential amino acid in the central nervous system. Glutamate receptors affect the survival and maturation of cortical, mesencephalic, and cerebellar granule neurons (Blandini *et al.*, 1996; Monti *et al.*, 2002; Hirasawa *et al.*, 2003), and play a central role in learning and memory. Ca^{2+} influx through glutamate receptors due to excitotoxic and ischemic damage can trigger multiple intracellular cascades and cause damage to neuronal cells in the brain (Choi, 1988; Tymianski, 1996; Ying *et al.*, 1997). Ionotropic glutamate receptors are mainly divided into two types, *N*-methyl-D-aspartate (NMDA) receptors and α -amino-3-hydroxy-5-methylisoxazole-4-propionic acid (AMPA) receptors. NMDA receptors are composed of an obligatory NR1 subunit and accessory subunits from the NR2 or NR3 family and the latter subunits are expressed differentially during development. Each subunit plays a specific role, contributing to the subcellular localization and channel properties of NMDA receptors (Luo *et al.*, 2011). Thus, changes of NMDA receptor subunit composition influence neuronal activity and survival. On the other hand, AMPA receptors are heteromeric complexes composed of four subunits (GluR1 to GluR4). Among the AMPA receptor subunits, GluR2 is expressed widely in hippocampal pyramidal and granule neurons (Hollmann and Heinemann, 1994) and in cortical neurons (Kondo *et al.*, 1997). AMPA receptor channel impermeability to Ca^{2+} is dependent upon the GluR2 subunit, and cells that contain AMPA receptor lacking the GluR2 subunit show high Ca^{2+} permeability and vulnerability to excitotoxicity (Liu and Zukin, 2007).

Lead is a potent, non-competitive and voltage-independent antagonist of NMDA receptor (Alkondon *et al.*, 1989). It is reported that lead binding at the Zn^{2+} -binding site of NMDA receptor is dependent on the receptor composition, i.e., lead showed competitive inhibition at the Zn^{2+} binding site of NR2A, but not at the Zn^{2+} binding site of NR2B (Gavazzo *et al.*, 2008). Moreover, lead alters NMDA receptor subunit composition. Expression of NR2A and NR1 is decreased (Nihei *et al.*, 2000) and the expression of NR1 splice variant mRNA is altered (Guilarte *et al.*, 2000) in rat hippocampus following exposure to lead. Further, lead exposure during synaptogenesis changes NMDA receptor expression at developing synapses (Neal *et al.*, 2011). Thus, lead-induced changes of NMDA receptor subunit composition may result in disruption of downstream signaling. However, the effects of lead on AMPA receptors have not been investigated. Therefore, in the present work, we investigated the effect of lead on the viability and GluR2 expression of prima-

ry-cultured rat cortical neurons to test our hypothesis that decreased GluR2 expression is involved in lead-induced neuronal cell death.

MATERIALS AND METHODS

Materials

Eagle's minimal essential salt medium (Eagle's MEM) was purchased from Nissui Pharmaceutical (Tokyo, Japan). Fetal calf serum (FCS) was purchased from Nichirei Biosciences Inc. (Tokyo, Japan). Horse serum (HS) was purchased from Gibco (Life Technologies, Carlsbad, CA, USA). Trypan blue, D-(+)-glucose, NaHCO_3 , sodium orthovanadate, phenylmethylsulfonyl fluoride (PMSF), sodium dodecyl sulfate (SDS), glycerol, and paraformaldehyde were purchased from Wako (Tokyo, Japan). Lead acetate was purchased from EBISU (Osaka, Japan). HEPES was purchased from DOJINDO (Kumamoto, Japan). L-Glutamine, arabinocytosine, formaldehyde and anti- β -actin antibody (AC-15) were purchased from Sigma-Aldrich (St. Louis, MO, USA). Pentobarbital was purchased from Kyoritsu (Tokyo, Japan). Bromophenol blue was purchased from Katayama Chemical Industries Co., Ltd. (Osaka, Japan). Tris-HCl, nonidet P-40, EDTA, mercaptoethanol and Protease Inhibitor Cocktail was purchased from Nacalai Tesque (Kyoto, Japan). Anti-GluR2 antibody (MAB397) was purchased from Millipore (Billerica, MA, USA). Anti-N-cadherin antibody (sc-7939) was purchased from Santa Cruz Biotechnology (Dallas, TX, USA).

Cell culture

The following procedures were performed under sterile conditions. The present study was approved by the university's animal ethics committee of Hiroshima University. Primary cultures were obtained from cerebral cortex of fetal rats at 18 days of gestation. Fetuses were taken from pregnant Slc:Wistar/ST rats under pentobarbital anesthesia. The prefrontal part of the cerebral cortex was dissected with a razor blade, and cells were dissociated by gentle pipetting. Dissociated cells were plated on culture plates (4×10^5 cells/cm²). Cultures were incubated in Eagle's MEM supplemented with 10% heat-inactivated FCS, L-glutamine (2 mM), D-(+)-glucose (11 mM), NaHCO_3 (24 mM), and HEPES (10 mM). Cultures were maintained at 37°C in an atmosphere of humidified 5% CO_2 in air. The cultures were incubated in MEM containing 10% FCS (days *in vitro* (DIV) 1-7) or 10% HS (DIV 8-11). The medium was exchanged every 2 days. Arabinocytosine (10 μM) was added to inhibit the proliferation of non-neuronal cells after DIV 6. Cultures were

Involvement of GluR2 decrease in lead-induced neuronal cell death

used for experiments at DIV 11. This protocol has been confirmed to produce cultures containing about 90% neurons by immunostaining for a neuron marker MAP2.

Treatment of cultures

Medium containing lead was changed at DIV 2, 4, 6, 8, and 10 and the neurons were exposed until DIV 11 for 9 days. In BDNF experiment, BDNF was added to the culture medium at DIV 2 and further added every day until DIV 10. Thus, the neurons were exposed also with BDNF for 9 days.

Trypan blue assay

After exposure to lead acetate, cell cultures were stained with 1.5% trypan blue for 10 min, then fixed with 10% formalin for 2 min, and rinsed with physiological saline. Unstained cells were regarded as viable and stained cells were regarded as dead. The viability of the cultures was calculated as the percentage ratio of the number of unstained cells to the total cells counted. Over 200 cells per cover slip were randomly counted.

LDH assay

LDH release was measured using a CytoTox 96 Non-Radioactive Cytotoxicity Assay (Promega®) according to the manufacturer's protocol. After exposure to lead acetate, culture medium (50 μ l) was transferred to a 96-well plate. Substrate mixture (50 μ l) was added to each well and allowed to react for 30 min in the dark at room temperature. Stop solution (50 μ l) was then added to each well, and the absorbance was read at 490 nm. The absorbance was normalized based on the absorbance of negative controls, which consisted of cells not exposed to lead.

Western blotting

After lead acetate treatment, cells were washed with PBS buffer and lysed in TNE buffer containing 50 mM Tris-HCl, 1% nonidet P-40, 20 mM EDTA, Protease Inhibitor Cocktail (1:200), 1 mM sodium orthovanadate, and 1 mM PMSF. The mixture was rotated at 4°C and centrifuged at 15,000 rpm, after which the supernatant was transferred to a microtube. The supernatant was added to sample buffer containing 100 mM Tris-HCl, 4% SDS, 20% glycerol, 0.004% bromophenol blue, and 5% mercaptoethanol, and then denatured at 95°C for 3 min. Protein was separated by SDS-polyacrylamide gel electrophoresis and transferred to a polyvinylidene difluoride membrane. The membrane was blocked with blocking buffer containing 5% skim milk for 1 hr, and then incubated with anti-GluR2 (1:2,000) and anti- β -actin (1:4,000) overnight, and with secondary antibody for 1 hr. Other

details were performed by the methods described previously (Hashida *et al.*, 2011). The protein was detected with an enhanced chemiluminescence detection system (Chemi-Lumi One L, Nacalai Tesque (Kyoto, Japan)). Quantitative analysis was performed with digital imaging software (Image J, NIH (Bethesda, MD, USA)), and GluR2 protein levels were corrected on the basis of β -actin protein levels.

Immunocytochemistry

Cells were seeded in poly-D-lysine-coated 8-well chamber slides (BD BioCoat™) and incubated overnight. After treatment with 5 and 20 μ M lead for 9 days, cells were washed with PBS(-) and fixed with 4% paraformaldehyde in PBS(-) for 15 min at room temperature. The slides were washed with PBS(-), blocked with 4 drops of Image-iT™ FX Signal Enhancer (Molecular Probes®) for 1 hr, and incubated with mouse anti-GluR2 (MAB397), which recognizes the N-terminal extracellular domain of GluR2 (1:250), and rabbit anti-N-cadherin (1:250) diluted in PBS(-) overnight at 4°C. Then, the slides were washed three times with PBS(-), and incubated with Alexa Fluor® 488-conjugated goat anti-mouse IgG (1:800, Molecular Probes®) and Alexa Fluor® 555-conjugated goat anti-rabbit IgG (1:800, Molecular Probes®) for 1 hr at room temperature in the dark. The slides were further washed three times with PBS(-), incubated with 4',6-diamidino-2-phenylindole dihydrochloride (DAPI, 1:2,000, Molecular Probes®) diluted in PBS(-) for 5 min, and washed again three times with PBS(-). Finally, the slides were enclosed in Prolong® Gold (Molecular Probes®) and observed under a confocal laser scanning microscope (Olympus, FV-1000-D).

Statistics

All the experiments were performed at least three times and representative data are shown. Data are expressed as mean + S.E.M. Statistical evaluation of the data was performed with ANOVA followed by Tukey's test. A value of $P < 0.05$ was considered to be indicative of significance.

RESULTS

Lead-induced cell death of cortical neurons

First, we investigated neuronal cell death induced by long-term exposure to lead. Rat cortical neurons were exposed to 5 and 20 μ M lead for 1, 3, 5, 7, and 9 days, and then the cell viability was examined by means of trypan blue assay (Fig. 1A) and LDH assay (Fig. 1B). Exposure of the cells to 5 μ M lead for 9 days resulted in a decrease of the cell viability to 29% of the control, while

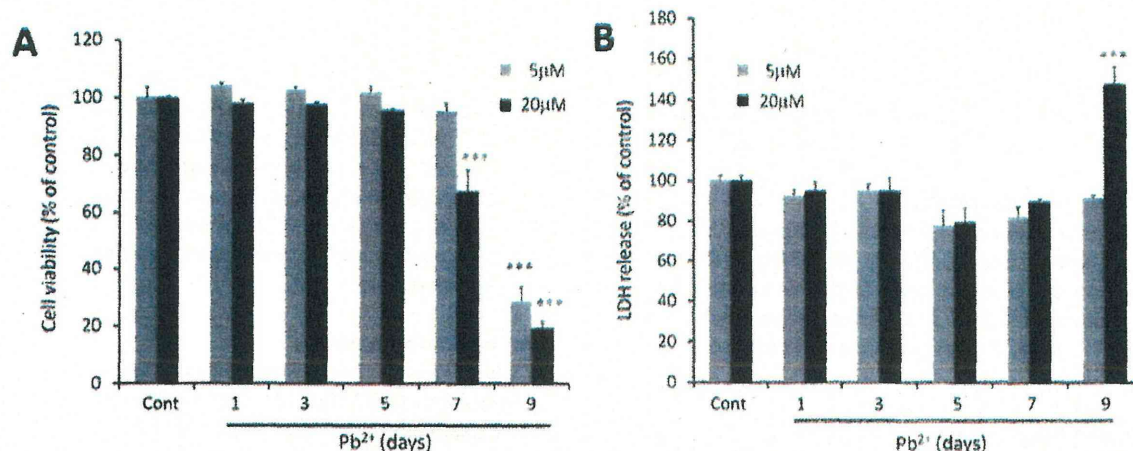


Fig. 1. Influence of long-term exposure to lead acetate (Pb^{2+}) on neurotoxicity. Cortical neurons were exposed to 5 and 20 μM Pb^{2+} for 1-9 days. Then cell viability was measured by means of trypan blue assay (A) and LDH assay (B). Data are expressed as mean + S.E.M. ($n = 4$). *** $P < 0.001$ vs. Cont.

exposure to 20 μM lead for 7 and 9 days decreased the cell viability to 67% and 19% of the control, respectively (Fig. 1A). Moreover, LDH release from cortical neurons was increased to 147% of the control after exposure to 20 μM lead for 9 days, although exposure to 5 μM lead had no effect (Fig. 1B).

Effect of long-term exposure of lead on GluR2 expression

We hypothesized that long-term exposure to lead would also decrease GluR2 expression, and would result in neuronal cell death. To examine this hypothesis, cortical neurons were exposed to 0.1-100 μM lead for 9 days and GluR2 protein expression was measured. As shown in Fig. 2A, a concentration-dependent decrease of GluR2 expression was seen upon exposure of the neurons to lead at concentrations above 1 μM and the decrease reached statistical significance at 5 μM . In 100 μM lead exposure, β -actin expression was also decreased, maybe due to drastic cell death (Fig. 2A). Moreover, cortical neurons were exposed to 5 and 20 μM lead for 1-9 days. A time-dependent decrease of GluR2 expression was observed in the neurons exposed to 5 and 20 μM lead. Exposure to 5 μM lead for 7 and 9 days significantly decreased the expression of GluR2 to 50% and 29% of the control (Fig. 2B), while exposure to 20 μM lead for 7 and 9 days significantly decreased the expression of GluR2 to 35% and 30% of the control (Fig. 2C). GluR2 subunits are largely expressed in cytoplasm, but some of them are

expressed in plasma membrane and act as components of AMPA receptors. Next, GluR2 expression at the plasma membrane was examined by immunocytochemistry (Fig. 3). Membrane expression of GluR2, which was confirmed by co-localization with N-cadherin, a membrane protein marker, was observed in the control cells. Exposure to 5 and 20 μM lead for 9 days markedly decreased GluR2 expression, in accordance with the result of western blotting (Fig. 2). Moreover, co-localization of GluR2 and N-cadherin was also considerably reduced, while intracellular distribution of GluR2 was not altered in these cells. These results suggest that exposure to lead decreases GluR2 expression, leading to a decrease in plasma membrane GluR2.

Amelioration of lead-induced GluR2 reduction and neuronal cell death by BDNF

It has been reported that BDNF potentially induces GluR2 promoter activity in SH-SY5Y cells, resulting in increased expression of GluR2 protein (Brené *et al.*, 2000). Thus, we tested whether BDNF also increased GluR2 protein expression in cortical neurons and ameliorated lead-induced neuronal cell death. Although the GluR2 protein level was not increased, the decrease of GluR2 expression induced by exposure to 5 and 20 μM lead was partly reversed by 50 ng/ml BDNF (Fig. 4A). Concomitantly, the decrease of cell viability caused by exposure to 5 and 20 μM lead was also significantly ameliorated by 50 ng/ml BDNF (Fig. 4B).

Involvement of GluR2 decrease in lead-induced neuronal cell death

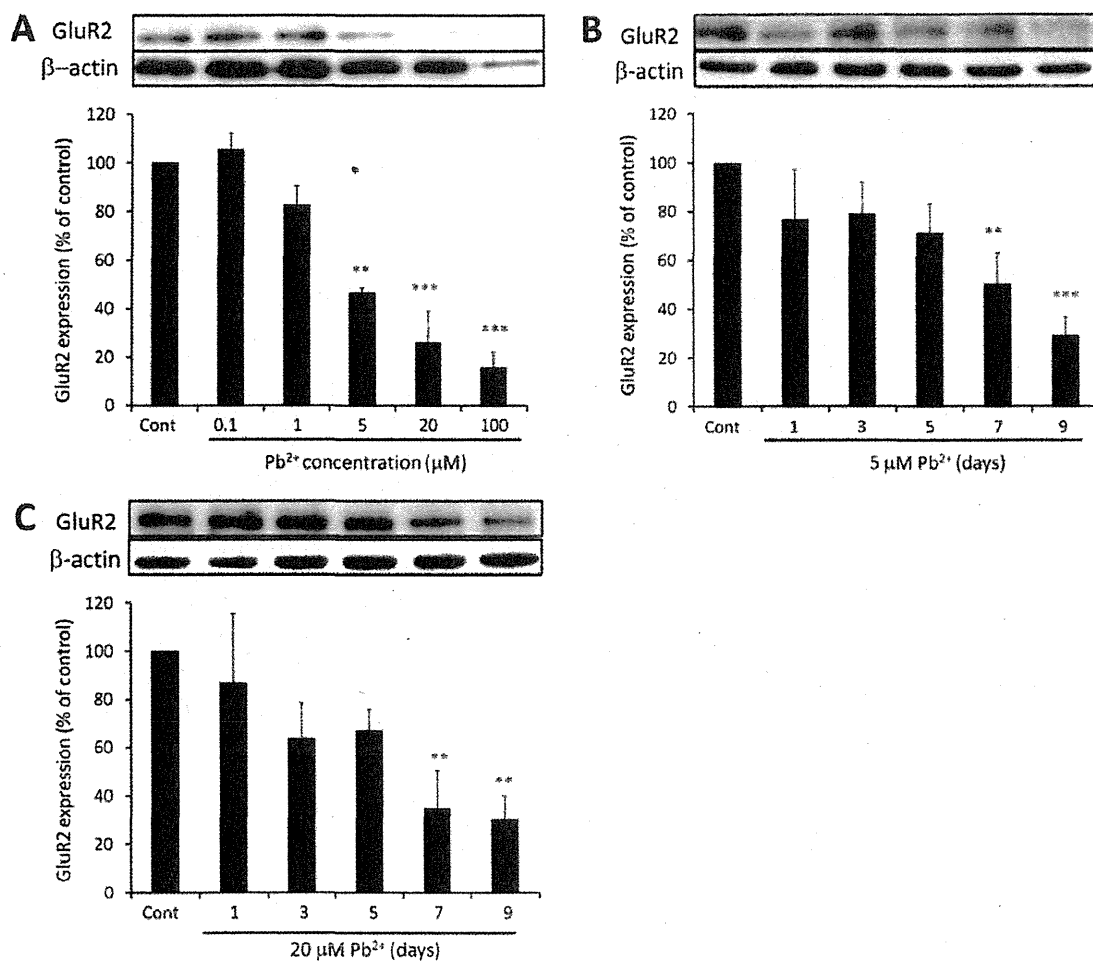


Fig. 2. Change of GluR2 protein expression induced by Pb^{2+} . Cortical neurons were exposed to 0.1-100 μM Pb^{2+} for 9 days (A), 5 μM Pb^{2+} for 1-9 days (B) and 20 μM (C) Pb^{2+} for 1-9 days, then GluR2 protein was detected by western blotting. Quantitative analysis was performed with Image J software and GluR2 protein levels were corrected on the basis of β -actin protein levels. Data are expressed as mean + S.E.M. (n = 3) **P < 0.01 vs. cont, ***P < 0.001 vs. cont.

DISCUSSION

In this study, cultured rat cortical neurons were exposed to lead to test our hypothesis that lead induces a decrease of GluR2 expression that in turn promotes neuronal cell death. We found that exposure to lead at 5-20 μM for 9 days decreased cell viability (Fig. 1A) and LDH release was increased after exposure to 20 μM lead for 9 days (Fig. 1B). Trypan blue-stained cells are regarded as dead, whereas LDH assay measures LDH release from membrane-disrupted cells. Thus, the differences in

evaluation of neuronal cell death between trypan blue assay and LDH assay is considered to be due to the different endpoints used to determine cell death in the two assays.

The expression of GluR2, an AMPA-type glutamate receptor subunit, was significantly decreased by exposure to 5-20 μM lead for 7 days (Fig. 2). It was reported that exposure to 0.1-10 μM lead for 48 hr decreased cell proliferation and increased caspase-3 activity in human SH-SY5Y neuroblastoma cells (Chetty *et al.*, 2005). Shinkai *et al.* (2010) reported that 5 μM lead induces endoplasmic

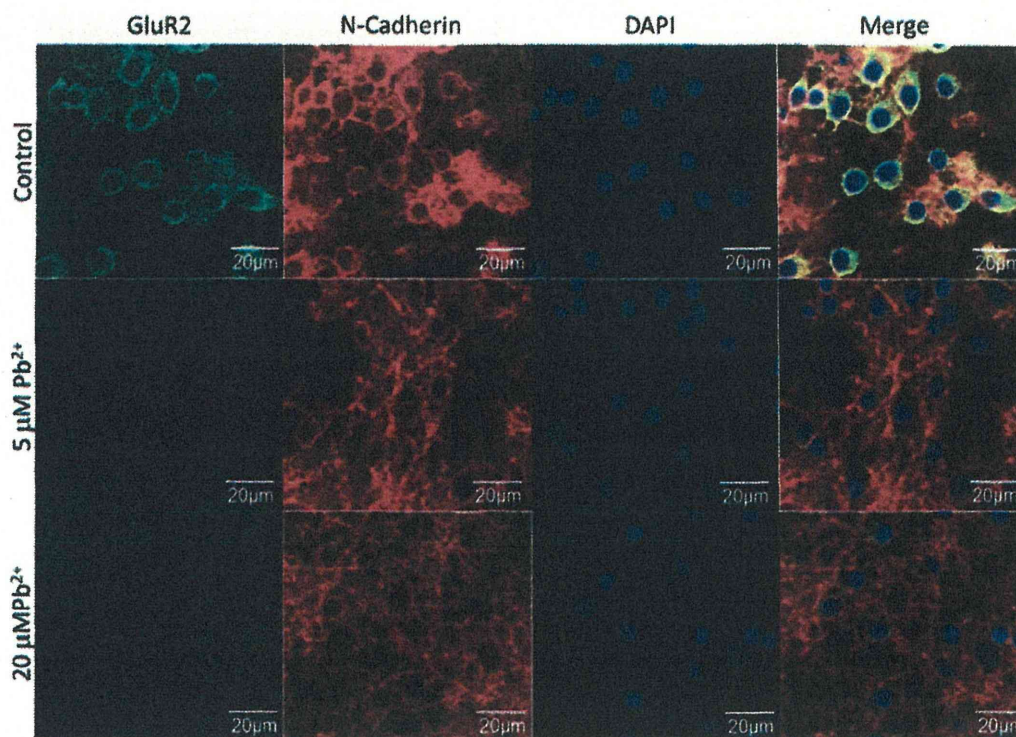


Fig. 3. Change of GluR2 protein expression on the plasma membrane induced by Pb^{2+} . Cortical neurons were exposed to 5 and 20 $\mu M Pb^{2+}$ for 9 days, and immunocytochemical staining was performed using a mouse anti-GluR2 antibody that recognizes the N-terminal extracellular domain of GluR2 (green) and a rabbit anti-N-cadherin antibody (red). Nuclear staining was performed using DAPI (blue). Yellow indicates colocalization between GluR2 and N-cadherin.

reticulum chaperones GRP78 and GRP94 via JNK-AP-1 pathway in vascular endothelial cells. Thus, the lead concentrations used in this study are similar to those used in other studies on the *in vitro* toxicities of lead. Incidentally, lead concentrations of up to 5 μM in blood have been reported in workers exposed to lead (Tomokuni *et al.*, 1993). It is well known that lead induces hematotoxicity by inhibiting the activity of enzymes involved in heme biosynthesis such as δ -aminolevulinic acid dehydratase. It is believed to be the most sensitive to lead (Bottomley and Muller-Eberhard, 1988). However, δ -aminolevulinic acid dehydratase is inhibited only in the presence of comparatively high lead concentrations of 0.1–1 mM in human erythroblastic cultures (Rio *et al.*, 2001). Thus, the concentrations used in this study are lower than those used in the above studies.

We have reported that long-term exposure of rat cortical neurons to tributyltin (TBT) decreases GluR2

expression, which results in increased Ca^{2+} permeability of AMPA receptors, because the Ca^{2+} permeability of AMPA receptors depends on whether or not they contain the GluR2 subunit (Nakatsu *et al.*, 2009). It was reported that GluR2 knockdown rats showed neuronal cell death in hippocampal CA1 and CA3, and the neuronal cell death was reduced by injection of Naspm (an open channel blocker selective for Ca^{2+} -permeable, GluR2-lacking AMPA receptors) and CNQX (a competitive blocker of AMPA receptors) (Oguro *et al.*, 1999), which suggests that GluR2 knockdown-induced neuronal cell death was mediated by Ca^{2+} -permeable, GluR2-lacking AMPA receptors. It has also been reported that knockdown of GluR2 exacerbates kainate-induced neuronal death (Friedman and Velísková, 1998; Friedman *et al.*, 2003). Iihara *et al.* (2001) suggested that kainate-induced neuronal cell death in GluR2 knockdown animals involves altered Na^{2+} permeability as well as altered Ca^{2+} permeability. It

Involvement of GluR2 decrease in lead-induced neuronal cell death

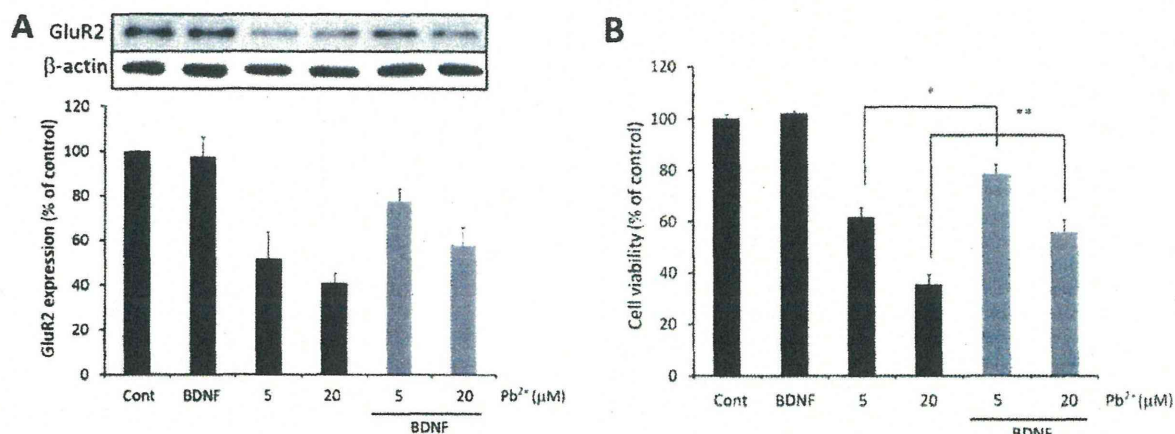


Fig. 4. Influence of exposure to BDNF on Pb^{2+} -induced decrease of GluR2 and neuronal cell death. Cortical neurons were exposed to 5 and 20 μM Pb^{2+} with or without 50 ng/ml BDNF for 9 days. (A) GluR2 protein was detected by western blotting. Quantitative analysis was performed with Image J software and GluR2 protein levels were corrected on the basis of β -actin protein levels. Data are expressed as mean + S.E.M. ($n = 4-5$). (B) Cell viability was measured by means of trypan blue assay. Data are expressed as mean + S.E.M. ($n = 8$). * $P < 0.05$, ** $P < 0.01$.

is known that GluR2 knockdown mice also show behavioral changes, such as impaired novelty-induced exploratory activities, disrupted motor coordination, and reduced self-directed behaviors, compared with control mice (Jia *et al.*, 1996). These findings are consistent with the idea that lead-induced GluR2 decrease can induce neuronal death via the increase of Ca^{2+} permeability of AMPA receptors. However, further studies are needed to measure lead-induced Ca^{2+} entry into neurons.

Expression of GluR2 can be induced by BDNF (Brené *et al.*, 2000), and one of the neuroprotective effects of BDNF is supposed to be mediated by recovery of GluR2. We also investigated whether increasing GluR2 expression by exposure to BDNF results in amelioration of lead-induced neuronal cell death. We found that the lead-induced GluR2 decrease was partly reversed and neuronal cell viability was increased by exposure to 50 ng/ml BDNF (Fig. 4). Because GluR2 levels are thought to reach plateau in primary cortical neurons, BDNF may not increase basal GluR2 expression. These results support the hypothesis that lead causes neuronal cell death through decreasing GluR2 protein expression, though BDNF might rescue lead-induced neuronal death by other mechanism such as an activation of PI3-kinase-Akt pathway (Hetman *et al.*, 1999). It should be confirmed that GluR2 overexpression recovers cell viability decreased by lead.

In conclusion, we investigated the influence of long-

term lead exposure on cultured cortical neurons. Lead induced a decrease of GluR2 protein and caused neuronal cell death. The decrease of GluR2 expression was considered to cause the lead-induced neuronal cell death, because cell viability was restored by BDNF treatment, which elicits a recovery of GluR2. A decrease in the population of GluR2-containing AMPA receptors is associated with increased Ca^{2+} influx. Our findings raise the possibility that GluR2 decrease in the brain is involved in lead-induced *in vivo* neurotoxicity, disorder of behavior, and impairment of cognitive function.

ACKNOWLEDGMENT

We thank the Analysis Center of Life Science, Hiroshima University for the use of their facilities. This work was supported by JSPS KAKENHI Grant Number 23310047 (to Y. Kotake).

REFERENCES

- Alkondon, M., Costa, A.C., Radhakrishnan, V., Aronstam, R.S. and Albuquerque, E.X. (1990): Selective blockade of NMDA-activated channel currents may be implicated in learning deficits caused by lead. *FEBS Lett.*, **261**, 124-130.
- Bellinger, D., Leviton, A., Allred, E. and Rabinowitz, M. (1994): Pre- and postnatal lead exposure and behavior problems in school-aged children. *Environ. Res.*, **66**, 12-30.
- Blandini, F., Porter, R.H. and Greenamyre, J.T. (1996): Glutamate

- and Parkinson's disease. *Mol. Neurobiol.*, **12**, 73-94.
- Bottomley, S.S. and Muller-Eberhard, U. (1988): Pathophysiology of heme synthesis. *Semin. Hematol.*, **25**, 282-302.
- Brené, S., Messer, C., Okado, H., Hartley, M., Heinemann, S.F. and Nestler, E.J. (2000): Regulation of GluR2 promoter activity by neurotrophic factors via a neuron-restrictive silencer element. *Eur. J. Neurosci.*, **12**, 1525-1533.
- Canfield, R.L., Gendle, M.H. and Cory-Slechta, D.A. (2004): Impaired neuropsychological functioning in lead-exposed children. *Dev. Neuropsychol.*, **26**, 513-540.
- Chetty, C.S., Vemuri, M.C., Campbell, K. and Suresh, C. (2005): Lead-induced cell death of human neuroblastoma cells involves GSH deprivation. *Cell. Mol. Biol. Lett.*, **10**, 413-423.
- Choi, D.W. (1988): Calcium-mediated neurotoxicity: relationship to specific channel types and role in ischemic damage. *Trends Neurosci.*, **11**, 465-469.
- Friedman, L.K., Segal, M. and Velísková, J. (2003): GluR2 knock-down reveals a dissociation between [Ca²⁺]_i surge and neurotoxicity. *Neurochem. Int.*, **43**, 179-189.
- Friedman, L.K. and Velísková, J. (1998): GluR2 hippocampal knockdown reveals developmental regulation of epileptogenicity and neurodegeneration. *Brain Res. Mol. Brain Res.*, **61**, 224-231.
- Froehlich, T.E., Lanphear, B.P., Auinger, P., Hornung, R., Epstein, J.N., Braun, J. and Kahn, R.S. (2009): Association of tobacco and lead exposures with attention-deficit/hyperactivity disorder. *Pediatrics*, **124**, e1054-e1063.
- Gavazzo, P., Zanardi, I., Baranowska-Bosiacka, I. and Marchetti, C. (2008): Molecular determinants of Pb²⁺ interaction with NMDA receptor channels. *Neurochem. Int.*, **52**, 329-337.
- Gracia, R.C. and Snodgrass, W.R. (2007): Lead toxicity and chelation therapy. *Am. J. Health Syst. Pharm.*, **64**, 45-53.
- Guilarte, T.R., McGlothlin, J.L. and Nihei, M.K. (2000): Hippocampal expression of N-methyl-D-aspartate receptor (NMDAR1) subunit splice variant mRNA is altered by developmental exposure to Pb(2+). *Brain Res. Mol. Brain Res.*, **76**, 299-305.
- Hashida, T., Kotake, Y. and Ohta, S. (2011): Protein disulfide isomerase knockdown-induced cell death is cell-line-dependent and involves apoptosis in MCF-7 cells. *J. Toxicol. Sci.*, **36**, 1-7.
- Hetman, M., Kanning, K., Cavanaugh, J.E. and Xia, Z. (1999): Neuroprotection by brain-derived neurotrophic factor is mediated by extracellular signal-regulated kinase and phosphatidylinositol 3-kinase. *J. Biol. Chem.*, **274**, 22569-22580.
- Hirasawa, T., Wada, H., Kohsaka, S. and Uchino, S. (2003): Inhibition of NMDA receptors induces delayed neuronal maturation and sustained proliferation of progenitor cells during neocortical development. *J. Neurosci. Res.*, **74**, 676-687.
- Hollmann, M. and Heinemann, S. (1994): Cloned glutamate receptors. *Annu. Rev. Neurosci.*, **17**, 31-108.
- Iihara, K., Joo, D.T., Henderson, J., Sattler, R., Taverna, F.A., Lourensen, S., Orser, B.A., Roder, J.C. and Tymianski, M. (2001): The influence of glutamate receptor 2 expression on excitotoxicity in GluR2 null mutant mice. *J. Neurosci.*, **21**, 2224-2239.
- Jia, Z., Agopyan, N., Miu, P., Xiong, Z., Henderson, J., Gerlai, R., Taverna, F.A., Velumian, A., MacDonald, J., Carlen, P., Abramow-Newerly, W. and Roder, J. (1996): Enhanced LTP in mice deficient in the AMPA receptor GluR2. *Neuron*, **17**, 945-956.
- Kjøller, C. and Diemer, N.H. (2000): GluR2 protein synthesis and metabolism in rat hippocampus following transient ischemia and ischemic tolerance induction. *Neurochem. Int.*, **37**, 7-15.
- Kondo, M., Sumino, R. and Okado, H. (1997): Combinations of AMPA receptor subunit expression in individual cortical neurons correlate with expression of specific calcium-binding proteins. *J. Neurosci.*, **17**, 1570-1581.
- Laidlaw, M.A., Mielke, H.W., Filippelli, G.M., Johnson, D.L. and Gonzales, C.R. (2005): Seasonality and children's blood lead levels: developing a predictive model using climatic variables and blood lead data from Indianapolis, Indiana, Syracuse, New York, and New Orleans, Louisiana (USA). *Environ. Health Perspect.*, **113**, 793-800.
- Lanphear, B.P., Hornung, R., Khoury, J., Yolton, K., Baghurst, P., Bellinger, D.C., Canfield, R.L., Dietrich, K.N., Bornschein, R., Greene, T., Rothenberg, S.J., Needleman, H.L., Schnaas, L., Wasserman, G., Graziano, J. and Roberts R. (2005): Low-level environmental lead exposure and children's intellectual function: an international pooled analysis. *Environ. Health Perspect.*, **113**, 894-899.
- Leviton, A., Bellinger, D., Allred, E.N., Rabinowitz, M., Needleman, H. and Schoenbaum, S. (1993): Pre- and postnatal low-level lead exposure and children's dysfunction in school. *Environ. Res.*, **60**, 30-43.
- Links, J.M., Schwartz, B.S., Simon, D., Bandeen-Roche, K. and Stewart, W.F. (2001): Characterization of toxicokinetics and toxicodynamics with linear systems theory: application to lead-associated cognitive decline. *Environ. Health Perspect.*, **109**, 361-368.
- Liu, S.J. and Zukin, R.S. (2007): Ca²⁺-permeable AMPA receptors in synaptic plasticity and neuronal death. *Trends Neurosci.*, **30**, 126-134.
- Luo, T., Wu, W.H. and Chen, B.S. (2011): NMDA receptor signaling: death or survival? *Front Biol.*, **6**, 468-476.
- Lustberg, M. and Silbergeld, E. (2002): Blood lead levels and mortality. *Arch. Intern. Med.*, **162**, 2443-2449.
- Monti, B., Marri, L. and Contestabile, A. (2002): NMDA receptor-dependent CREB activation in survival of cerebellar granule cells during *in vivo* and *in vitro* development. *Eur. J. Neurosci.*, **16**, 1490-1498.
- Nakatsu, Y., Kotake, Y., Takishita, T. and Ohta, S. (2009): Long-term exposure to endogenous levels of tributyltin decreases GluR2 expression and increases neuronal vulnerability to glutamate. *Toxicol. Appl. Pharmacol.*, **240**, 292-298.
- Neal, A.P., Worley, P.F. and Guilarte, T.R. (2011): Lead exposure during synaptogenesis alters NMDA receptor targeting via NMDA receptor inhibition. *Neurotoxicology*, **32**, 281-289.
- Nihei, M.K., Desmond, N.L., McGlothlin, J.L., Kuhlmann, A.C. and Guilarte, T.R. (2000): N-methyl-D-aspartate receptor subunit changes are associated with lead-induced deficits of long-term potentiation and spatial learning. *Neuroscience*, **99**, 233-242.
- Oguro, K., Oguro, N., Kojima, T., Grooms, S.Y., Calderone, A., Zheng, X., Bennett, M.V. and Zukin, R.S. (1999): Knockdown of AMPA receptor GluR2 expression causes delayed neurodegeneration and increases damage by sublethal ischemia in hippocampal CA1 and CA3 neurons. *J. Neurosci.*, **19**, 9218-9227.
- Rio, B., Froquet, R. and Parent-Massin, D. (2001): In vitro effect of lead acetate on human erythropoietic progenitors. *Cell. Biol. Toxicol.*, **17**, 41-50.
- Shinkai, Y., Yamamoto, C. and Kaji, T. (2010): Lead induces the expression of endoplasmic reticulum chaperones GRP78 and GRP94 in vascular endothelial cells via the JNK-AP-1 pathway. *Toxicol. Sci.*, **114**, 378-386.
- Tomokuni, K., Ichiba, M. and Fujishiro, K. (1993): Interrelation between urinary delta-aminolevulinic acid (ALA), serum ALA,

Involvement of GluR2 decrease in lead-induced neuronal cell death

- and blood lead in workers exposed to lead. *Ind. Health*, **31**, 51-57.
- Tymianski, M. (1996): Cytosolic calcium concentrations and cell death *in vitro*. *Adv. Neurol.*, **71**, 85-105.
- Ying, H.S., Weishaupt, J.H., Grabb, M., Canzoniero, L.M., Sensi, S.L., Sheline, C.T., Monyer, H. and Choi, D.W. (1997): Sublethal oxygen-glucose deprivation alters hippocampal neuronal AMPA receptor expression and vulnerability to kainate-induced death. *J. Neurosci.*, **17**, 9536-9544.

AMP-activated protein kinase-mediated glucose transport as a novel target of tributyltin in human embryonic carcinoma cells†

Cite this: DOI: 10.1039/c3mt20268b

Shigeru Yamada,^a Yaichiro Kotake,^b Yuko Sekino^a and Yasunari Kanda^{*a}

Organotin compounds such as tributyltin (TBT) are known to cause various forms of cytotoxicity, including developmental toxicity and neurotoxicity. However, the molecular target of the toxicity induced by nanomolar levels of TBT has not been identified. In the present study, we found that exposure to 100 nM TBT induced growth arrest in human pluripotent embryonic carcinoma cell line NT2/D1. Since glucose provides metabolic energy, we focused on the glycolytic system. We found that exposure to TBT reduced the levels of both glucose-6-phosphate and fructose-6-phosphate. To investigate the effect of TBT exposure on glycolysis, we examined glucose transporter (GLUT) activity. TBT exposure inhibited glucose uptake via a decrease in the level of cell surface-bound GLUT1. Furthermore, we examined the effect of AMP-activated protein kinase (AMPK), which is known to regulate glucose transport by facilitating GLUT translocation. Treatment with the potent AMPK activator, AICAR, restored the TBT-induced reduction in cell surface-bound GLUT1 and glucose uptake. In conclusion, these results suggest that exposure to nanomolar levels of TBT causes growth arrest by targeting glycolytic systems in human embryonic carcinoma cells. Thus, understanding the energy metabolism may provide new insights into the mechanisms of metal-induced cytotoxicity.

Received 28th December 2012,
Accepted 20th February 2013

DOI: 10.1039/c3mt20268b

www.rsc.org/metallomics

Introduction

Growing evidence suggests that environmental metals contribute to developmental toxicity and neurotoxicity.^{1–3} Since the developing brain is inherently more vulnerable to injury than the adult brain, exposure to metals during early fetal development can potentially cause neurological disorders at doses much lower than those that are toxic in adults.^{4–7} Therefore, it is necessary to elucidate the cytotoxic effects of such metals at low levels.

Organotin compounds are well known to cause cytotoxicity. Although organotin compounds or derivatives have been shown to have a potential anti-tumor activity^{8,9} and some of them have already been entered into preclinical trials,¹⁰ tributyltin (TBT) is considered to be associated with developmental toxicity and neurotoxicity.¹¹ For example, TBT can cause increased fetal mortality, decreased fetal birth weights, and behavioral abnormalities in rat offspring.^{12,13} TBT is known to affect

fertilization and embryonic development.¹⁴ Moreover, TBT has been shown to induce neuronal death by glutamate excitotoxicity in cultured rat cortical neurons.¹⁵ Although the use of TBT has already been restricted, butyltin compounds, including TBT, have been reported to be still present at concentrations between 50 and 400 nM in human blood.¹⁶ However, the mechanism by which nanomolar levels of TBT cause cytotoxicity is not fully understood.

Glucose is the primary energy source for homeostasis. Glucose transport across the plasma membrane *via* a glucose transporter (GLUT) is a rate-limiting step in glucose metabolism.¹⁷ AMP-activated protein kinase (AMPK), a serine threonine kinase, has been shown to regulate glucose uptake by facilitating the translocation of the GLUT to the membrane or by activation of transporter activity at the plasma membrane.^{18,19} The fetal brain has been reported to rely on anaerobic glycolysis to meet its energy demands.²⁰ Thus, GLUT is considered essential in the early organogenesis period. GLUT1, a major subtype of GLUT in fetal tissue, has been shown to mediate organogenesis in rat embryos.²¹ In addition, clinical data regarding human GLUT1 deficiency syndrome suggest that GLUT1 is necessary for human brain development.²²

In the present study, we hypothesized a possible link between TBT toxicity and glucose metabolism. We found that

^a Division of Pharmacology, National Institute of Health Sciences, 1-18-1, Kamiyoga, Setagaya-ku 158-8501, Japan. E-mail: kanda@nihs.go.jp; Fax: +81-3-3700-9704; Tel: +81-3-3700-9704

^b Department of Xenobiotic Metabolism and Molecular Toxicology, Graduate School of Biomedical and Health Sciences, Hiroshima University, Japan

† Electronic supplementary information (ESI) available. See DOI: 10.1039/c3mt20268b

exposure to TBT reduced the amounts of glucose-6-phosphate and fructose-6-phosphate *via* a decrease in surface-bound GLUT1 in the human pluripotent embryonic carcinoma cell line NT2/D1. In addition, treatment with the potent AMPK activator, 5-aminoimidazole-4-carboxamide ribonucleoside (AICAR), restored the inhibitory effect of TBT on both cell surface-bound GLUT1 levels and glucose uptake. We report here that the glycolytic pathway is a molecular target of nanomolar levels of TBT in human embryonic carcinoma cells.

Methods

Cell culture

NT2/D1 cells were obtained from the American Type Culture Collection. The cells were cultured in Dulbecco's modified Eagle's medium (DMEM; Sigma-Aldrich, St. Louis, MO, USA) supplemented with 10% fetal bovine serum (FBS; Biological Industries, Ashrat, Israel) and 0.05 mg mL⁻¹ penicillin-streptomycin mixture (Life Technologies, Carlsbad, CA, USA) at 37 °C and 5% CO₂. For neural differentiation, all-trans retinoic acid (RA; Sigma-Aldrich) was added to the medium twice a week at a final concentration of 10 μM.

Cell proliferation assay

Cell viability was measured using the CellTiter 96 Aqueous One Solution Cell Proliferation Assay (Promega, Madison, WI, USA), according to the manufacturer's instructions. Briefly, NT2/D1 cells were seeded into 96-well plates and exposed to different concentrations of TBT. After exposure to TBT, One Solution Reagent was added to each well, and the plate was incubated at 37 °C for another 2 h. Absorbance was measured at 490 nm using an iMark microplate reader (Bio-Rad, Hercules, CA, USA).

Glucose uptake assay

A glucose uptake assay was performed using a fluorescent glucose derivative, 2-[N-(7-nitrobenz-2-oxa-1,3-diazol-4-yl)amino]-2-deoxy-D-glucose (2-NBDG; Peptide Institute Inc., Osaka, Japan) by the previously reported procedure with slight modifications.²³ Briefly, NT2/D1 cells exposed to TBT were incubated with 2-NBDG (100 μM) for 2 h at 37 °C. The 2-NBDG uptake reaction was stopped by draining the incubation medium and washing the cells twice with ice-cold PBS. The incorporated 2-NBDG was measured using a Wallac1420ARVO fluoroscan (Perkin-Elmer, Waltham, MA, USA) with excitation at 488 nm and emission at 515 nm. The fluorescence intensities were normalized to the total protein content.

Hexokinase activity assay

Hexokinase activity was determined using a commercial Hexokinase Colorimetric Assay Kit (Biovision, Mountain View, CA, USA), according to the manufacturer's instructions.

AMPK activity assay

AMPK activity was determined using a commercial CycLex AMP Kinase Assay Kit (MBL International, Woburn, MA, USA), according to the manufacturer's instructions.

Determination of glucose-6-phosphate and fructose-6-phosphate

Intracellular metabolites were extracted and used for subsequent capillary electrophoresis time-of-flight mass spectrometry (CE-TOFMS) analysis, as described previously.²⁴ Glucose-6-phosphate and fructose-6-phosphate were determined using an Agilent CE capillary electrophoresis system (Agilent Technologies, Waldbronn, Germany) equipped with an Agilent G3250AA LC/MSD TOF system (Agilent Technologies, Palo Alto, CA), an Agilent 1100 series isocratic HPLC pump, a G1603A Agilent CE-MS adapter kit, and a G1607A Agilent CE-electrospray ionization 53-MS sprayer kit. For system control and data acquisition, G2201AA Agilent ChemStation software was used for CE, and Agilent TOF (Analyst QS) software was used for TOFMS.

Western blotting

Western blotting was performed as previously reported.²⁵ Briefly, the cells were lysed using Cell Lysis Buffer (Cell Signaling Technology, Danvers, MA, USA), and proteins were then separated by sodium dodecyl sulfate (SDS)-polyacrylamide gel electrophoresis and electrophoretically transferred to Immobilon-P membranes (Millipore, Billerica, MA, USA). The membranes were probed using primary antibodies (anti-GLUT1 polyclonal antibodies [1:200; Santa Cruz Biotechnology, Santa Cruz, CA, USA], anti-c-Myc polyclonal antibodies [1:1000; Sigma-Aldrich], anti-Flag monoclonal antibodies [1:1000; Sigma-Aldrich], and anti-β-actin monoclonal antibodies [1:1000; Sigma-Aldrich]). The membranes were then incubated with secondary antibodies against rabbit or mouse IgG conjugated with horseradish peroxidase (Cell Signaling Technology). The bands were visualized using an ECL Western Blotting Analysis System (GE Healthcare, Buckinghamshire, UK), and images were acquired using a LAS-3000 Imager (Fujifilm UK Ltd., Systems, Bedford, UK). The density of each band was quantified with ImageJ software (NIH, Bethesda, MD, USA).

Cell surface biotinylation

NT2/D1 cell surface proteins were biotinylated using a Cell Surface Protein Isolation Kit, according to the manufacturer's instructions (Pierce, Rockford, IL, USA). Briefly, cells were incubated with ice-cold phosphate-buffered saline (PBS; pH 7.4) containing Sulfo-NHS-SS-Biotin, with gentle rocking for 30 min at 4 °C. The biotinylated proteins were precipitated with streptavidin beads and eluted from the beads with SDS sample buffer. The proteins were analyzed by western blotting with anti-GLUT1 antibodies.

Immunohistochemistry

Cells, cultured on glass coverslips, were fixed in 4% paraformaldehyde in PBS (pH 7.4) for 15 min at room temperature. The fixed cells were incubated with anti-GLUT1 polyclonal antibodies (1:100; Santa Cruz) for 1 h at room temperature. Finally, they were incubated with Alexa488-conjugated secondary antibodies (1:200; Life Technologies) for 1 h at room temperature. The cells were enclosed in SlowFade (Life Technologies) and examined under a BIOREVO BZ-9000 fluorescent microscope (Keyence, Osaka, Japan).

Transfection

Cells were transiently transfected with Flag-tagged GLUT1 in pEF6 (a kind gift from Dr Rathmell) and c-Myc-tagged constitutively active-AMPK- α 1 (T172D) or c-Myc-tagged dominant-negative-AMPK- α 1 (K45R) in pcDNA3 (a kind gift from Dr Carling) using the FuGene HD Transfection Reagent (Promega), according to the manufacturer's protocol. After 48 h incubation, the transfectants were cultured with 12.5 $\mu\text{g mL}^{-1}$ blasticidin or 0.5 mg mL^{-1} G418.

Real-time PCR

After total RNA was isolated from NT2/D1 cells using TRIzol (Life Technologies), quantitative real-time reverse transcription (RT)-PCR with a QuantiTect SYBR Green RT-PCR Kit (QIAGEN, Valencia, CA, USA) was performed using an ABI PRISM 7900HT sequence detection system (Applied Biosystems, Foster City, CA, USA), as previously reported.²⁶ The relative changes in the amounts of transcripts in each sample were normalized using ribosomal protein L13 (RPL13) mRNA levels. The sequences of the primers used for real-time PCR analysis are as follows: GLUT1 (forward, 5'-CCAGCTGCCATTGCCGTT-3'; reverse, 5'-GACGTAGGGACCA-CACAGTTGC-3'), GLUT2 (forward, 5'-CACACAAGACCTGGAA-TTGACA-3'; reverse, 5'-CGGTCATCCAGTGGAAACAC-3'), GLUT3 (forward, 5'-CAATGCTCCTGAGAAGATCATAA-3'; reverse, 5'-AAA-GCGGTTGACGAAGAGT-3'), GLUT4 (forward, 5'-CTGGGCTCA-CAGTGCTAC-3'; reverse, 5'-GTCAGGCGCTTCAGACTCTT-3'), nestin (forward, 5'-GGCAGCGTTGGAACAGAGGT-3'; reverse, 5'-CATCTTGAGGTGCGCCAGCT-3'), NeuroD (forward, 5'-GGAAA-CGAACCCACTGTGCT-3'; reverse, 5'-GCCACACAAATTCGTGGT-G-3'), Math1 (forward, 5'-GTCCGAGCTGCTACAACG-3'; reverse, 5'-GTGGTGGTGGTTCGCTTTT-3'), MAP2 (forward, 5'-CCAATGG-ATTCCCATACAGG-3'; reverse, 5'-CTGCTACAGCCTCAGCAGTG-3'), RPL13 (forward, 5'-CATCGTGGCTAAACAGGTACTG-3'; reverse, 5'-GCACGACCTTGAGGGCAGCC-3').

Materials

TBT was obtained from Tokyo Chemical Industry (Tokyo, Japan). Tin acetate (TA), AICAR, and rosiglitazone were obtained from Sigma-Aldrich. All other reagents were of analytical grade and obtained from commercial sources.

Statistical analysis

All data were presented as mean \pm S.D. ANOVA followed by a *post hoc* Tukey test was used to analyze data in Fig. 1–4. Unpaired Student's *t* test was used to analyze data in Fig. 5. A *p* value of less than 0.05 was considered significant.

Results

To examine the effect of TBT on the proliferation of human NT2/D1 embryonic carcinoma cells, we exposed the cells to different concentrations of TBT for 24 h and measured cell viability by MTT assay. Treatment with TBT reduced cell viability in a dose-dependent manner (Fig. 1A; 0.03–0.3 μM). We observed that almost all cells were detached from the

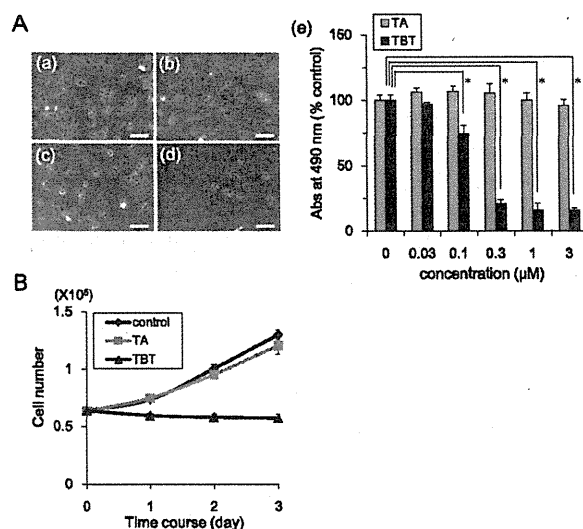


Fig. 1 Effect of TBT exposure on cell proliferation in NT2/D1 cells. (A) NT2/D1 cells were seeded into 96-well plates and exposed to TBT at different concentrations for 24 h. (a–d) Phase-contrast photomicrographs of NT2/D1 cells exposed to TBT at 0, 0.03, 0.1, or 0.3 μM (Bar = 100 μm). (e) Cell viability in the presence of TBT or TA was examined using the CellTiter 96 Aqueous One Solution Cell Proliferation Assay. (B) NT2/D1 cells (6×10^5 cells) were seeded into 100 mm dishes and exposed to 100 nM TBT. After 24, 48, and 72 h, cell count was determined using a hemocytometer. **P* < 0.05.

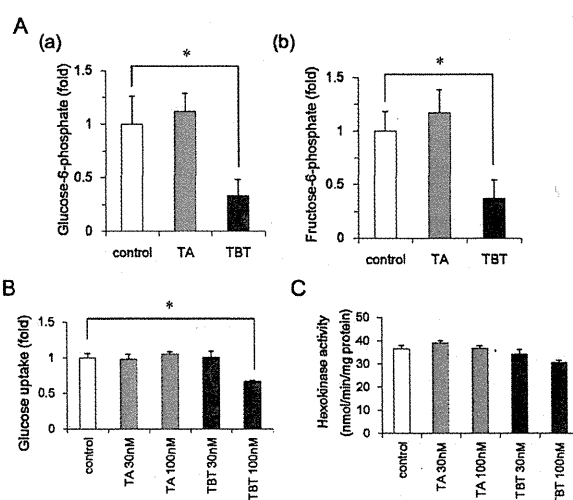


Fig. 2 Effect of TBT exposure on glycolytic systems in NT2/D1 cells. (A) After 24 h exposure to 100 nM TBT or TA, glucose 6-phosphate (a) and fructose 6-phosphate (b) levels were determined using CE-TOFMS. (B) After exposure to TBT or TA (30, 100 nM) for 24 h, glucose uptake assay was performed using a fluorescent glucose analog 2-NBDG. The fluorescence intensities of incorporated 2-NBDG were normalized to total cellular protein content. (C) After exposure to TBT or TA (30, 100 nM) for 24 h, hexokinase activity was measured using a commercial assay kit. **P* < 0.05.

culture dish at TBT concentrations of 300 nM and above. In contrast, the less toxic TA had little effect at any concentration (Fig. 1A–e). We performed time-course experiments with 100 nM TBT, and determined the cell number. Exposure to